


Rapamycin-based graft-versus-host disease prophylaxis increases the immunosuppressivity of myeloid-derived suppressor cells without affecting T cells and anti-tumor cytotoxicity

J. Scheurer ,* T. Reisser,*
F. Leithäuser,[†] J. J. Messmann,*
K. Holzmann,[‡] K.-M. Debatin* and
G. Strauss*

*Department of Pediatrics and Adolescent
Medicine, University Medical Center Ulm,

[†]Institute of Pathology, University Ulm, and

[‡]Genomic-Core Facility, University Ulm, Ulm,
Germany

Summary

The immunosuppressant rapamycin (RAPA) inhibits mammalian target of rapamycin (mTOR) functions and is applied after allogeneic bone marrow transplantation (BMT) to attenuate the development of graft-versus-host disease (GVHD), although the cellular targets of RAPA treatment are not well defined. Allogeneic T cells are the main drivers of GVHD, while immunoregulatory myeloid-derived suppressor cells (MDSCs) were recently identified as potent disease inhibitors. In this study, we analyzed whether RAPA prevents the deleterious effects of allogeneic T cells or supports the immunosuppressive functions of MDSCs in a BMT model with major histocompatibility complex (MHC) classes I and II disparities. RAPA treatment efficiently attenuated clinical and histological GVHD and strongly decreased disease-induced mortality. Although splenocyte numbers increased during RAPA treatment, the ratio of effector T cells to MDSCs was unaltered. However, RAPA treatment induced massive changes in the genomic landscape of MDSCs preferentially up-regulating genes responsible for uptake or signal transduction of lipopeptides and lipoproteins. Most importantly, MDSCs from RAPA-treated mice exhibited increased immunosuppressive potential, which was primarily inducible nitric oxide synthase (iNOS)-dependent. Surprisingly, RAPA treatment had no impact on the genomic landscape of T cells, which was reflected by unchanged expression of activation and exhaustion markers and cytokine profiles in T cells from RAPA-treated and untreated mice. Similarly, T cell cytotoxicity and the graft-versus-tumor effect were maintained as co-transplanted tumor cells were efficiently eradicated, indicating that the immunosuppressant RAPA might be an attractive approach to strengthen the immunosuppressive function of MDSCs without affecting T cell immunity.

Keywords: GVHD, allogeneic bone marrow transplantation, GVT effect, MDSCs, rapamycin

Accepted for publication 7 July 2020

Correspondence: G. Strauss, Medical Center
Ulm, Department of Pediatrics and
Adolescent Medicine, Eythstraße 24,
89075 Ulm, Germany.

E-mail: gudrun.strauss@uniklinik-ulm.de

Introduction

Graft-versus-host disease (GVHD) still represents the major complication after allogeneic bone marrow transplantation (BMT), resulting in life-threatening complications for the recipient. GVHD occurs when T cells in the transplant become activated by alloantigens and subsequently destroy recipient tissues. However, allogeneic T cells are required for residual tumor eradication [= graft-versus-tumor (GVT) effect] [1]. Therefore, GVHD therapies must comply with

the requirements to reduce the risk of target tissue destruction while maintaining T cell immunity and GVT activity.

The macrolide rapamycin (RAPA) is known for its immunosuppressive properties, as it inhibits mTOR (mammalian target of rapamycin), a master regulator of protein synthesis, metabolism, proliferation and differentiation. mTOR exists in two independent cellular multi-protein complexes – mTORC1 and mTORC2. RAPA forms a complex with its intracellular receptor FK506-binding protein (FKBP12) to specifically inhibit mTORC1.

RAPA effects on mTORC2 are variable, and require prolonged treatment [2,3]. mTOR activity affects differentiation and functions of various innate and adaptive immune cells involved in GVHD development. Activity of the mTOR complex is vital for the differentiation of CD4⁺ T helper type (Th)1, Th2 and Th17 subsets and effector CD8⁺ T cells [4,5], as well as for the maturation of dendritic cells [6]. The induction of immunosuppressive cells, however, requires mTOR inactivity. *De-novo* differentiation of regulatory T cells (T_{regs}) *in vivo* and *in vitro* is supported by RAPA [4,7,8]. Recently, an activating effect of RAPA on the organ-specific recruitment, expansion and activation of myeloid-derived suppressor cells (MDSCs), a subset of immune suppressive cells of myeloid origin, was also reported [9–13], although few studies describe the requirement of mTOR activity for MDSC functionality [14–17].

Murine MDSCs, which develop under inflammatory conditions, are characterized by granulocyte marker 1 (Gr-1) and CD11b expression and subdivided into two subsets, depending on the Gr-1 epitope [lymphocyte antigen 6 (Ly-6)C or Ly-6G] expressed. Monocytic (mMDSC; CD11b⁺Ly6G⁺Ly6C^{high}) as well as granulocytic (gMDSC; CD11b⁺Ly6G⁺Ly6C^{low}) MDSCs preferentially interfere with T cell activation, proliferation, homing and function. MDSCs immunosuppressive mechanisms are versatile, and include the deprivation of amino acids required for T cell activity by enzymes such as inducible nitric oxide synthase (iNOS), arginase 1 and indoleamine 2,3-dioxygenase (IDO) or the production of immunosuppressive cytokines [interleukin (IL)-10 and transforming growth factor (TGF)- β] [18–20].

Because MDSCs and RAPA procure immunosuppressive effects on the immune response, both are attractive candidates for GVHD prevention and might mutually influence each other. mTOR inhibitors have been registered for the successful clinical use in solid organ transplantations [21–23] and are introduced as a therapeutic alternative in the management of GVHD in combination therapies, but are used extremely rarely as a front-line GVHD therapy [24]. Cellular therapy with MDSCs in murine BMT models is extremely efficient in preventing GVHD [25–27], although clinical trials are currently missing. However, a good correlation between MDSC accumulation and alleviated GVHD is reported in humans [28,29]. Similarly, MDSCs accumulate after allogeneic BMTs in mice [30,31], but their immunosuppressive capacity is not sufficient for GVHD prevention.

GVHD development after BMT is dependent upon the activation status, the numbers and interplay of all cells contributing positively or negatively to GVHD development. Therefore, it is highly relevant to define the cellular targets of RAPA to improve its clinical

application. Using an allogeneic BMT mouse model, in which RAPA treatment prevents GVHD development, we could show that RAPA does not abrogate T cell functions, but enhances the immunosuppressive capacity of MDSCs.

Material and methods

Bone marrow transplantation (BMT)

Female C57BL/6 (B6; H-2^b, CD45.2), B6D2F1 (H-2^{bxd}, CD45.2) (Janvier, Le Genest-Saint-Isle, France), B6.SJL-Ptprc^aPepc^b/BoyJ (B6.SJL; H-2^b, CD45.1) mice (breeding pairs from The Jackson Laboratory and bred at Ulm University, Germany) were used (9–20 weeks of age). One day before BMT, mice were irradiated with 12 Gy split into two doses 3 h apart using a ¹³⁷Cs source. T cell depletion (TCD) of BM was performed according to Messmann *et al.* [25]. Mice were reconstituted with 5×10^6 TCD-BM in the presence or absence of 2×10^7 spleen cells (SC). Rapamycin (Rapamune) (Pfizer, New York City, NY, USA) diluted in 1 \times PBS was injected intraperitoneally (i.p.) with a concentration of 1.5 mg/kg/mouse every second day until day 10 and twice weekly until the end of the experiment; 1×10^4 P815 tumor cells/mouse were injected intravenously (i.v.) at the day of BMT. GVHD development was assessed according to Cooke *et al.* [32] by evaluating the clinical parameters weight loss, activity, posture, fur texture and skin integrity. Animals euthanized during the experiment due to their moribund state remained included in the calculation until the end of experiment with their final GVHD scores. All animal experiments were performed according to the international regulations for the care and use of laboratory animals and were approved by the local Ethical Committee Regierungspräsidium, Tübingen, Germany.

Histology

Organs were fixed in 4% formalin, paraffin-embedded and slide sections were stained with hematoxylin and eosin. A pathologist who was blinded for the experimental history examined skin, intestine and liver for histopathology. Histopathology of GVHD was graded according to Kaplan *et al.* [33].

Tissue preparation

Spleen. Splenic single-cell suspensions were prepared by pouring the spleen through a cell strainer (pore size 70 μ m), followed by erythrocyte depletion.

Liver. For liver cell isolation, the liver was perfused by the injection of 5 ml liver perfusion medium (GIBCO, Carlsbad, CA, USA), followed by 5 ml liver digest medium (GIBCO)

into the vena cava inferior. After removing the gall bladder, liver was digested for 30 min at 37°C in 10 ml liver digest medium. Afterwards, liver cell suspension was prepared by pouring the liver through a cell strainer (pore size 70 µm). Liver cells were suspended in 35% Percoll (Sigma-Aldrich, St Louis, MO, USA), followed by overlaying cells onto 70% Percoll and centrifuging the Percoll gradient at 13RCF (g) for 20 min. Liver leukocytes were collected from the interface and residual erythrocytes were depleted.

Serum. Serum was prepared from submandibular blood to which cytokine stabilization buffer (U-CyTech Biosciences, Utrecht, the Netherlands) was added. Serum samples were stored at -80°C until ProcartaPlex Multiplex immunoassays (Thermo Fisher Scientific, Waltham, MA, USA) were performed.

Serum cytokine analysis

Serum cytokine concentrations were determined by ProcartaPlex Multiplex immunoassay (Thermo Fisher Scientific) and analyzed on a BIO-RAD Bioplex 200 system (Bio-Rad, Hercules, CA, USA).

Isolation of MDSCs

MDSCs were isolated from single-cell suspensions of spleen or liver by magnetic activated cell sorting using CD11b MicroBeads (Miltenyi, Bergisch Gladbach, Germany) according to the manufacturer's protocol. Purity ranged between 80 and 95%.

CD3⁺ T cell sorting

Splenic single-cell suspensions were stained with anti-CD3-specific antibodies followed by fluorescence activated cell sorting (FACS) using a FACSAriaTM II flow cytometer (BD Biosciences, Franklin Lakes, NJ, USA). Purity was > 90%.

Flow cytometry

A total of 5×10^5 – 1×10^6 cells were stained with antibodies listed in Supporting information, Table S1. T_{regs} were detected by surface staining of CD4, CD25 followed by fixation, permeabilization and intracellular forkhead box protein 3 (FoxP3) staining using the FoxP3 transcription factor staining buffer kit (Thermo Fisher Scientific). For intracellular pS6 staining, cells were fixed with 4% paraformaldehyde and lysed with 0.1% saponin (Sigma-Aldrich). pS6 was determined using phospho-S6 ribosomal protein (Ser235/236) antibody (Cell Signaling Technology, Danvers, MA, USA) and detected by using a fluorescein isothiocyanate (FITC)-coupled anti-rabbit secondary antibody (Santa Cruz Biotechnology, Dallas, TX, USA). Flow cytometric analyses were performed on a LSR II flow cytometer (BD Biosciences, Franklin Lakes, NJ, USA).

Cell culture conditions

Tumor cell lines. P815 and EL-4 tumor cell lines were cultured in RPMI-1640 (GIBCO), 10% fetal calf serum (Sigma Aldrich), 2 mM L-glutamine (GIBCO), 1 mM sodium pyruvate (GIBCO) at 37°C and 7.5% CO₂.

Mixed lymphocyte reaction. MLRs were performed in α-minimum essential medium (Lonza, Basel, Switzerland), 10% fetal calf serum (Sigma Aldrich), 2 mM L-glutamine (GIBCO), 1 mM sodium pyruvate (GIBCO), 100 U/ml penicillin-streptomycin (GIBCO) and 0.05 mM 2-mercaptoethanol (GIBCO) at 37 °C and 7.5% CO₂.

Chromium release assay. Chromium release assays were performed in RPMI-1640 (GIBCO), 10% fetal calf serum (Sigma Aldrich), 2 mM L-glutamine (GIBCO), 1 mM sodium pyruvate (GIBCO), 100 mM HEPES (Biochrom, Berlin, Germany) at 37°C and 7.5% CO₂.

Carboxyfluorescein diacetate succinimidyl ester (CFSE) labeling

A total of 2×10^6 cells/ml were labeled with 5 µM carboxyfluorescein succinimidyl ester (CFSE) (Thermo Fisher Scientific) for 10 min at 37°C followed by washing steps with ice-cold phosphate-buffered saline (PBS)-5% fetal calf serum (FCS).

Mixed lymphocyte reaction (MLR)

A total of 2.5×10^5 CFSE-labeled B6.SJL-derived SCs were stimulated with 2.5×10^5 irradiated B6D2F1-derived SCs (33 Gy) in the absence or presence of MDSCs. iNOS was inhibited using 500 µM L-N^G-monomethyl-L-arginine-citrate (L-NMMA) (Merck, Darmstadt, Germany). T cell proliferation was determined after 4 days using flow cytometry [% T cell suppression = 100% - (proliferation effector T cells + stimulator T cells + MDSCs)/% proliferation effector T cells + stimulator T cells × 100].

Chromium release assay

Cytotoxic capacity of T cells was determined by chromium release assays according to Strauss *et al.* [34]; 5×10^3 tumor cells labeled with 100 µCi ⁵¹Cr were co-cultured with spleen cells at different effector : target cell ratios. After 6 h the supernatant was assayed for ⁵¹Cr release in a Top CountNXT counter (Packard BioScience, Meriden, CT, USA) [% specific release = (experimental release - spontaneous release)/(maximum release - spontaneous release) × 100].

Quantitative reverse transcription-polymerase chain reaction (qRT-PCR)

qRT-PCR was performed using the SsoAdvancedTM Universal SYBR[®] Green Supermix (Bio-Rad). The expression

of target genes was determined using the comparative C_T method. Mouse aryl hydrocarbon receptor-interacting protein (AIP) was used as housekeeping gene. Primer sets used are listed in Supporting information, Table S2. Analysis was performed on a CFX Connect Optics Module (Bio-Rad).

Microarray analysis

Microarray analyses. Microarray analyses were performed using 200 ng total RNA as starting material and 5.5 μ g ssDNA per hybridization (GeneChip Fluidics Station 450; Affymetrix, Santa Clara, CA, USA). Total RNAs were amplified and labeled following the Whole Transcript (WT) Sense Target Labeling Assay (<http://www.affymetrix.com>). Labeled ssDNA was hybridized to Mouse Gene 1.0 ST Affymetrix GeneChip arrays (Affymetrix). The chips were scanned with an Affymetrix GeneChip Scanner 3000 and subsequent images analyzed using Affymetrix[®] Expression Console™ Software (Affymetrix).

Transcriptome analyses. Transcriptome analyses were performed using BRB-ArrayTools developed by Dr Richard Simon and BRB-ArrayTools Development Team (<http://linus.nci.nih.gov/BRB-ArrayTools.html>). Raw feature data were normalized and \log_2 intensity expression summary values for each probe set were calculated using robust multi-array average [35].

Filtering. Genes showing minimal variation across the set of arrays were excluded from the analysis. Genes whose expression differed by at least 1.5-fold from the median in at least 20% of the arrays were retained.

Class comparison. Genes were identified as differentially expressed among the two classes using a two-sample *t*-test. Genes were considered statistically significant if their *P*-value was less than 0.05 and displayed a fold change between the two groups of at least 1.5-fold. Benjamini and Hochberg correction was used to provide 90% confidence that the false discovery rate was less than 10% [36].

Gene ontology analysis of differentially expressed genes. GoMINER analysis tool was used to identify the most affected biological processes, as defined by Gene Ontology annotation. Complete microarray data are available at Gene Expression Omnibus (GEO accession number: GSE141416).

Statistics

Data were analyzed using the Mann–Whitney test or unpaired Student's *t*-test. For multiple comparisons analysis of variance (ANOVA), Tukey's multiple comparison test or Kruskal–Wallis test were used. The log-rank (Mantel–Cox)

test was used for survival studies. Results were considered as significant if $P < 0.05$. Statistical tests were performed with GraphPad Prism version 8.

Results

Rapamycin treatment attenuates GVHD in a parent into F1 mismatched BMT mouse model

To validate the therapeutic effect of RAPA in preventing GVHD, we used a parent into F1 BMT mouse model with major histocompatibility complex (MHC) classes I and II disparities of 50%. Lethally irradiated B6D2F1 (H-2^{bxd}) recipient mice were reconstituted with TCD-BM alone or together with SCs from B6 mice (H-2^b). RAPA treatment started on the day of BMT and was repeated every second day during the first 10 days, followed by twice-weekly injections until the end of the experiment. Transplantation of TCD-BM and SCs induced severe clinical GVHD with tissue damage in intestine, liver and skin, which resulted in a mortality rate of approximately 90% in PBS-treated mice. Importantly, RAPA treatment rescued survival to about 75%, associated with alleviated histological GVHD, especially in intestine and skin. Mice reconstituted with TCD-BM alone were disease-free due to the absence of allogeneic T cells in the transplant (Fig. 1a,b). Altogether, these data clearly indicate that RAPA treatment starting on the day of BMT strongly attenuates GVHD and rescues survival in approximately 75% of transplanted mice.

Rapamycin treatment increases splenic leukocyte numbers without altering the distribution of leukocyte subsets

RAPA-mediated GVHD inhibition can be due to either a decrease and inactivation of alloantigen-specific T cells or an increase of immunosuppressive cells. Therefore, the cellular composition in spleen and the GVHD target organ liver of RAPA-treated mice was compared to PBS-treated controls. Total splenocytes, including CD4⁺ and CD8⁺ T cells, T_{regs} and MDSCs, significantly increased 10 days after BMT in RAPA-treated mice compared to PBS-treated mice (Fig. 2a). Total MDSC numbers were defined by the expression of Gr-1 and CD11b (Supporting information, Fig. S1a), while T_{regs} were detected in the CD4⁺CD25⁺ population by FoxP3 expression (Supporting information, Fig. S1b). Percentages of CD4⁺, CD8⁺ T cells, T_{regs} and MDSCs, however, were comparable between both groups (Fig. 2a). No increase of total leukocytes or individual leukocyte subsets was detected in the liver upon RAPA treatment (Fig. 2b).

MDSCs are composed of mMDSCs (CD11b⁺Ly-6G^{neg}Ly-6C^{high}) and gMDSCs (CD11b⁺Ly-6G^{pos}Ly-6C^{low}) (Supporting

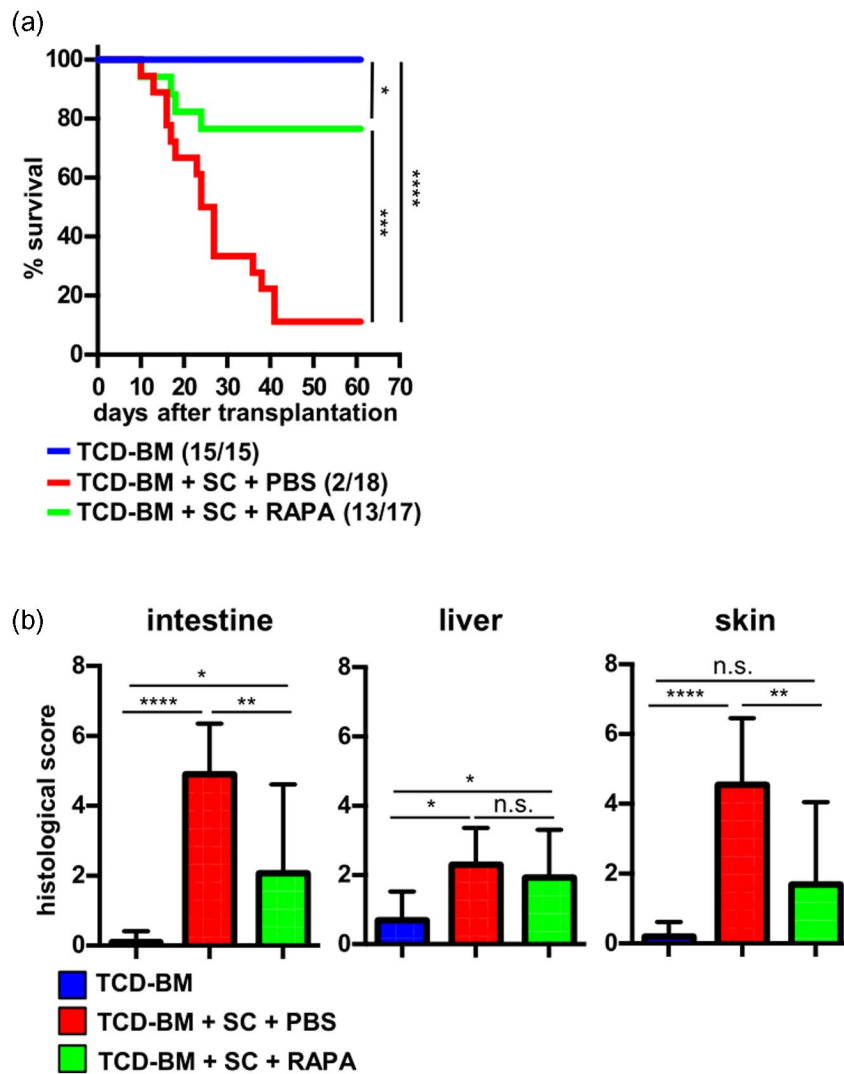


Fig. 1. Rapamycin (RAPA) treatment attenuates graft-versus-host disease (GVHD) in a major histocompatibility complex (MHC) classes I and II mismatched B6 into the F1 bone marrow transplant (BMT) model. Lethally irradiated B6D2F1-recipient mice (H-2^{bx/d}) were reconstituted with T cell depletion bone marrow (TCD-BM) from B6 mice (H-2^b) in the presence or absence of B6-derived spleen cells (SCs). RAPA or phosphate-buffered saline (PBS) intraperitoneal (i.p.) injections were administered every second day during the first 10 days, followed by a treatment twice weekly until the end of the experiment. (a) Survival was determined. Surviving animals/total animals treated are indicated in brackets. (b) Paraffin sections of intestine (ileum and colon), liver and skin of 10–13 animals/group were analyzed for histological GVHD on the day mice were euthanized due to their moribund state or at the end of the experiment. (a) Kaplan–Meier method and log-rank test. (b) Analysis of variance (ANOVA) Tukey's multiple comparison test. * $P \leq 0.05$; ** $P \leq 0.01$; *** $P \leq 0.001$; **** $P \leq 0.0001$; n.s. = not significant.

information, Fig. S1c). Although RAPA treatment increased MDSC numbers, the distribution of both subpopulations in spleen and liver was unchanged. The majority of MDSCs were gMDSCs represented in spleen with approximately 60% and in liver greater than 70%. mMDSCs represented up to 40% of splenic MDSCs and up to 30% of liver MDSCs (Fig. 2c).

Overall, these results indicate that RAPA treatment leads to leukocyte expansion at least in the spleen without affecting leukocyte distribution.

T cell responses are not affected by rapamycin treatment

As RAPA strongly attenuated GVHD development, but did not affect the numbers of allogeneic T cells, we questioned whether T cell functions such as activation, cytokine secretion or cytotoxicity of T cells were altered. RAPA treatment did not alter the percental distribution of activation markers CD25 and CD69 of CD4⁺ and CD8⁺ T cells and the induction of effector memory T cells (CD44^{high}, CCR7⁻, CD62L⁻)

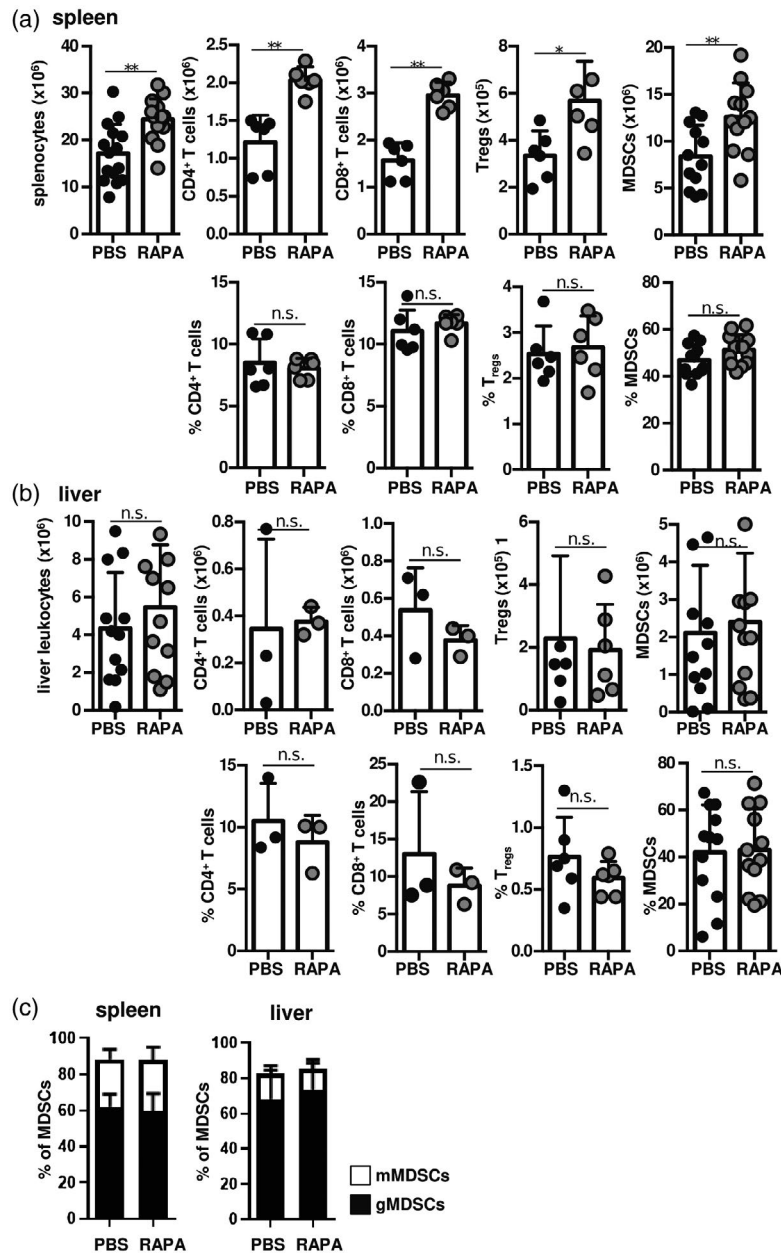


Fig. 2. Rapamycin (RAPA) increases splenic leukocyte numbers without altering the distribution of leukocyte populations. Lethally irradiated B6D2F1-recipient mice (H-2^{bxd}) were reconstituted with T cell depletion bone marrow (TCD-BM) from B6 mice (H-2^b) together with B6-derived spleen cells (SCs). RAPA or phosphate-buffered saline (PBS) intraperitoneal (i.p.) injections were administered every second day. Ten days after bone marrow transplant (BMT), splenocytes (a) and liver leukocytes (b) were determined and analyzed for absolute numbers and percentage of CD4⁺ and CD8⁺ T cells, regulatory T cells (T_{reg}) and myeloid-derived suppressor cells (MDSCs). (c) Percentage of monocytic (m-) and granulocytic (g-) MDSCs in spleen and liver were determined by staining infiltrated MDSCs for CD11b, Ly-6C and Ly-6G. (a–c) Data represent the mean value ± standard deviation (s.d.). (a,b) Total splenocyte and liver lymphocyte numbers of 12–15 animals/group were analyzed. T cells subsets of three to six animals/group and MDSCs of 12 animals/group were analyzed. (c) Six animals/group were analyzed. (a,b) Mann-Whitney test. *P ≤ 0.05; **P ≤ 0.01; n.s. = not significant.

(Fig. 3a). Adhesion and homing molecules CCR9, LPAM-1, LFA-1 and CXCR3 of CD4⁺ and CD8⁺ T cells exhibited no differences in expression in RAPA and PBS-treated mice (Fig. 3b). Also, the expression density of all analyzed markers was unchanged (Supporting information, Fig. S2).

Persistent T cell activation is often associated with T cell exhaustion. However, no differences in the expression of exhaustion markers of CD4⁺ and CD8⁺ T cells from RAPA or PBS-treated mice were detected. CD4⁺ T cells strongly up-regulated programmed cell death 1 (PD-1), B and T

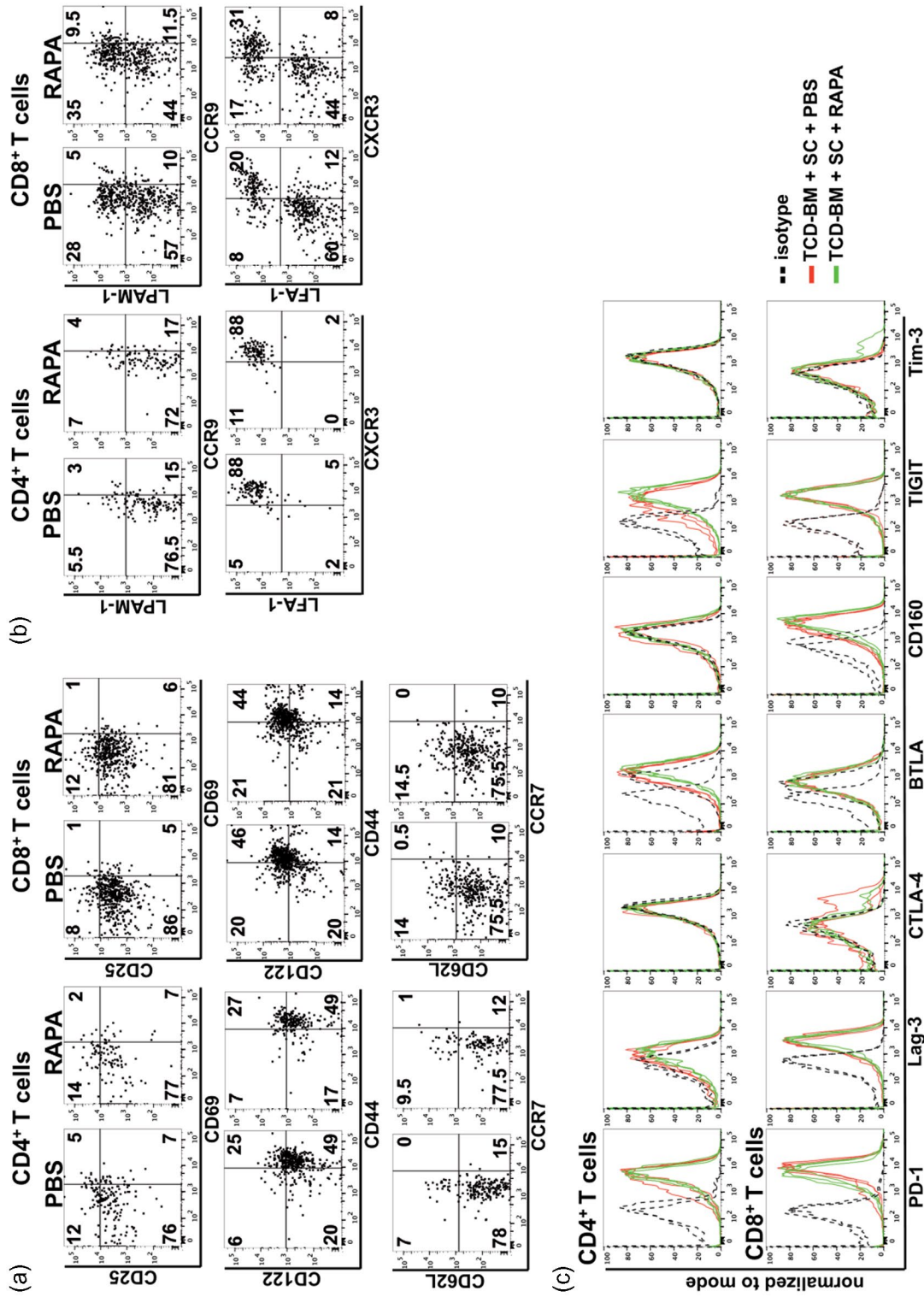


Fig. 3. Graft-versus-host disease (GVHD) prophylaxis by rapamycin does not affect T cell activation. (a–c) Lethally irradiated B6D2F1-recipient mice (H-2^{bkd}) were reconstituted with T cell depletion bone marrow (TCD-BM) from B6 mice (H-2^b) together with B6-derived spleen cells (SCs). RAPA or phosphate-buffered saline (PBS) intraperitoneal (i.p.) injections were administered every second day. Ten days after BMT, splenic CD4⁺ and CD8⁺ T cells were stained for (a) activation, (b) homing and adhesion or (c) exhaustion markers. (a,b) Graphs are representative for one of three mice analyzed/group. (c) Fluorescence activated cell sorting (FACS) diagrams are representative for three of six mice analyzed in each group.

lymphocyte attenuator (BTLA) and T cell immunoglobulin and immunoreceptor tyrosine-based inhibition motif domain (TIGIT), and showed low lymphocyte-activation gene 3 (Lag-3) expression. Consistent with a more pronounced increase of CD8⁺ memory cells (CD122⁺CD44⁺) more exhaustion markers (PD-1, Lag-3, BTLA, CD160 and TIGIT) were up-regulated on CD8⁺ T cells compared to CD4⁺ T cells. Cytotoxic T lymphocyte antigen 4 (CTLA-4) and T-cell immunoglobulin and mucin-domain containing-3 (Tim-3) expression was marginally detectable on both T cell subsets (Fig. 3c). Although the induction of T helper type 2/T cytotoxic type (Th2/Tc2) cells is associated with disease-free progression after BMT, RAPA did not affect the Th1/Tc1 and Th2/Tc2 balance. Isolated splenic T cells from RAPA and PBS-treated mice exhibited similar mRNA expression levels of Th1/Tc1-associated [tumor necrosis factor (TNF)- α , interferon (IFN)- γ and IL-2] and Th2/Tc2-associated cytokines (IL-4, -5, -10, -13) 10 days after BMT (Fig. 4a). Simultaneously, no differences in mRNA expression levels of transcription factors indispensable for type 1 [signal transducer and activator of transcription 4 (STAT-4), T-bet] or type 2 [STAT-6, GATA binding protein 3 (GATA-3)] T cells were detectable (Fig. 4b). This result was further confirmed by comparable serum cytokine concentrations of TNF- α , IFN- γ , IL-4, IL-5 and IL-13 in RAPA and PBS-treated mice. Solely, serum IL-2 decreased upon RAPA treatment (Fig. 4c).

To further clarify whether and how RAPA treatment affects T cells in the context of BMT, we performed microarray analysis and compared gene expression profiles of sorted splenic CD3⁺ T cells from RAPA- and PBS-treated mice. Surprisingly, at a false discovery rate (FDR) level of 0.1 (FC > 1.5 \times) gene array analysis showed no differences in gene expression profiles of T cells between RAPA- and PBS-treated mice, with the exception of the gene encoding for glucagon-like peptide 1 receptor (Glp1r) (FDR: 0.0544). Even without applying a correction for multiple testing, only 11 genes were differentially expressed ($P < 0.05$, FC > 1.5 \times) in T cells upon RAPA treatment (Fig. 4d,e, Supporting information, Table S3). As a correction for multiple testing is sometimes too stringent with small sample sizes, we also checked for protein–protein interaction within this set of 11 genes using the STRING database [37]. Because no interactions between any of these genes were revealed, it is very unlikely that this set of genes represents true differential regulation based upon RAPA treatment. Overall, these data indicate that RAPA-induced GVHD inhibition is not mediated by expression changes in the T cell compartment.

Rapamycin treatment increases the immunosuppressive potential of MDSCs

As RAPA was recently identified to improve MDSC functions in autoimmunity and solid organ transplantation

[9,10,12,13], we examined the effect of RAPA on the immunosuppressive potential of MDSCs induced in the context of allogeneic BMT. Therefore, splenic MDSCs (CD11b⁺Gr-1⁺) of RAPA- and PBS-treated recipient mice (H-2^b, CD45.2) were isolated 10 days after BMT and were co-cultured with CFSE-labeled B6.SJL-derived spleen cells (H-2^b, CD45.1) stimulated with irradiated allogeneic B6D2F1-derived spleen cells (H-2^{bxd}, CD45.2) *in vitro*. MDSCs from RAPA-treated mice exhibited an increased immunosuppressive capacity towards alloantigen-stimulated CD45.1⁺CD3⁺ T cells (Fig. 5a). Analysis of mRNA expression levels of immunosuppressive molecules revealed a strong increase of iNOS and elevated expression of IDO and slightly increased expression of arginase 1 in RAPA-activated MDSCs. Other immunosuppressive factors and cytokines, such as HO1, COX2, TGF- β and IL-10, were equally expressed compared to MDSCs from PBS-treated mice (Fig. 5b). iNOS inhibitor L-NMMA totally abrogated the suppressive potential of RAPA-activated MDSCs towards alloantigen-stimulated T cells, indicating a major role of iNOS in the immunosuppressive potential (Fig. 5c). To define the effects of RAPA on MDSC functions, microarray analysis of isolated splenic MDSCs from RAPA- and PBS-treated mice were performed. Volcano plot analysis of MDSCs showed impressive differences in the gene expression profile of RAPA-activated MDSCs compared to MDSCs derived from PBS-treated mice (Fig. 5d). In total, 179 genes were differentially expressed (FDR < 0.1, FC > 1.5 \times), from which 133 genes were up-regulated and 46 genes were down-regulated in RAPA-activated MDSCs (Fig. 5e). By enrichment analysis of target genes using the GO database, we identified the top 10 changed GO terms and linked target genes, which are listed in Table 1. Preferentially, genes associated with the uptake or cellular responses to lipopeptides, lipoproteins and lipoteichoic acids such as Toll-like receptor 1 (TLR-1), CD36 or CD14 were strongly up-regulated in RAPA-activated MDSCs, suggesting that these receptors contribute to the increased immunosuppressive capacity. To verify that RAPA directly targets MDSCs, we determined intracellular pS6 expression in MDSCs 1 h after PBS and RAPA application in mice transplanted with allogeneic BM and SCs. MDSCs isolated from RAPA-treated mice showed strongly reduced pS6 expression compared to MDSCs derived from PBS-treated mice (Fig. 5f). In accordance with minimal genomic changes in T cells after RAPA treatment, RAPA hardly affected the pS6 expression of isolated T cells from BM-transplanted mice (Supporting information, Fig. S3). In summary, these data clearly show that RAPA directly targets MDSCs and thereby supports their immunosuppressive potential.

Rapamycin treatment does not abrogate the GVT effect after allogeneic BMT

Maintenance of the GVT effect is the major therapeutic goal of allogeneic hematopoietic stem cell transplantation

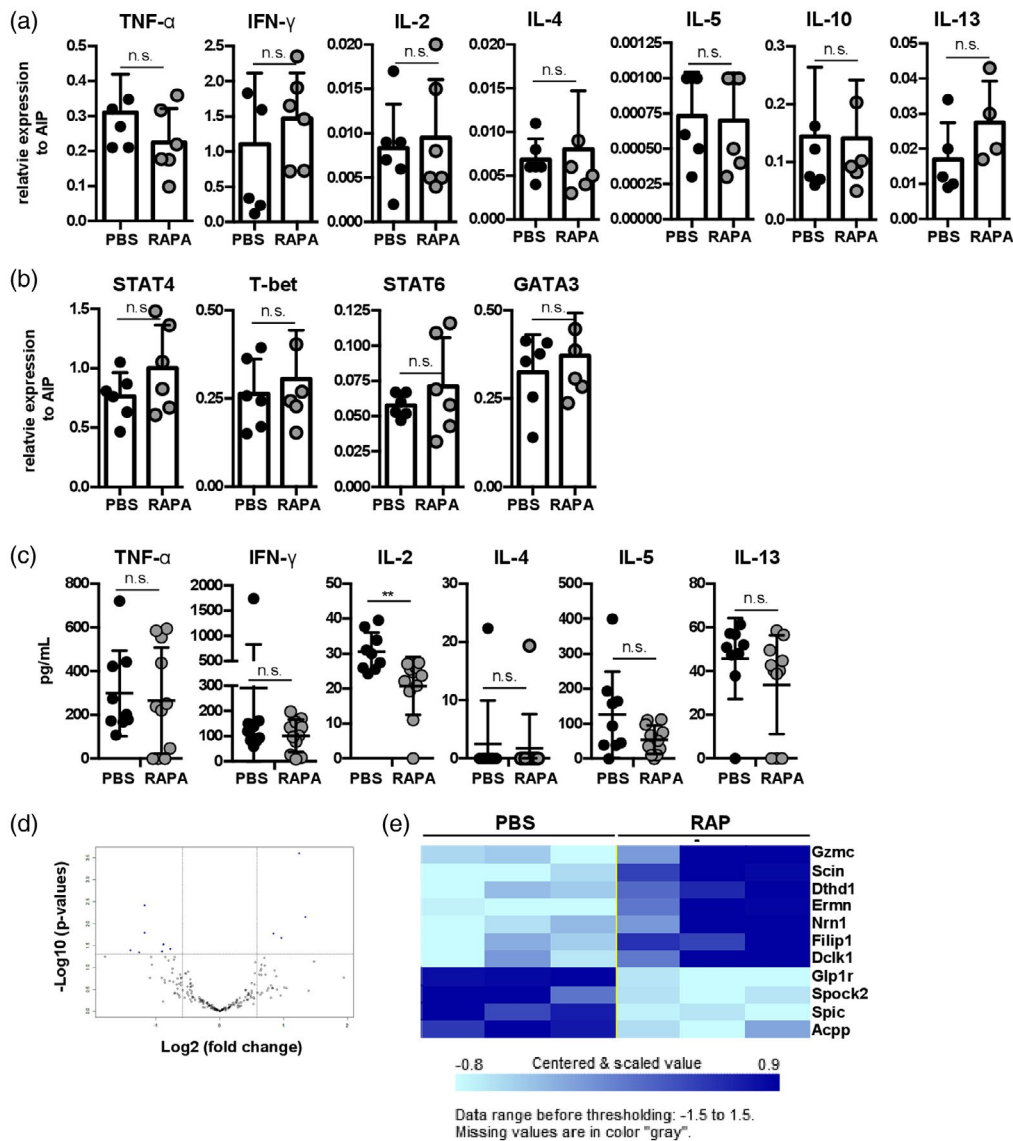


Fig. 4. T cells of rapamycin-treated mice exhibit unchanged cytokine profiles and no differences in gene expression. (a–e) Lethally irradiated B6D2F1-recipient mice (H-2^{bxd}) were reconstituted with T cell depletion bone marrow (TCD-BM) from B6 mice (H-2^b) together with B6-derived spleen cells (SCs). RAPA or phosphate-buffered saline (PBS) intraperitoneal (i.p.) injections were administered every second day until day 10 post-transplantation. (a,b) CD3⁺ T cells were isolated from spleens and quantitative reverse transcription–polymerase chain reactions (qRT-PCRs) of (a) type 1 [tumor necrosis factor (TNF)- α , interferon (IFN)- γ , interleukin (IL)-2], type 2 (IL-4, -5, -10, -13)-associated cytokines and (b) transcription factors were performed. Relative expression to aryl hydrocarbon receptor-interacting protein (AIP) was calculated. (c) Serum concentrations of types 1 and 2-associated cytokines were determined. (d) Volcano plot comparing gene expression of *ex-vivo*-isolated splenic T cells from RAPA or PBS-treated mice. Blue dots represent genes scored as differentially expressed between both groups. They display large magnitude fold changes (*x*-axis) and high statistical significance [$-\log_{10}$ of *P*-value (*y*-axis)]. Unfilled black dots show genes having a *P*-value > 0.05 and fold change less than 2 ($\log_2 = 1$). (e) Heat-map of differentially expressed genes between splenic T cells from RAPA or PBS-treated mice. Data represent the mean value \pm standard deviation (s.d.) of four to six mice/group (a,b) and of nine to 11 mice/group (c). (d,e) Data represent three mice analyzed/group. (a–c) Mann–Whitney test. **P* \leq 0.01; n.s. = not significant.

in the treatment of hematopoietic tumors. Therefore, splenic T cells from RAPA- and PBS-treated mice were analyzed for their cytotoxic potential 10 days after BMT. RNA expression of cytotoxic molecules perforin and granzyme B (Gzmb) and death-inducing TNF-related apoptosis-inducing (TRAIL)

and CD95L ligands were even slightly up-regulated in T cells from RAPA-treated animals (Fig. 6a). Most importantly, cytotoxic capacity of splenic T cells from RAPA-treated mice was not impaired compared to T cells isolated from PBS-treated mice. The alloantigen expressing P815 mastocytoma

tumor cell line (H-2^d) was efficiently lysed, while the syngeneic T cell lymphoma cell line EL-4 (H-2^b) was not recognized (Fig. 6b), further supporting our findings that RAPA treatment does not affect the functionality of T cells. As RAPA did not abrogate T cell cytotoxicity *in vitro*, the GVT

effect under RAPA treatment was analyzed *in vivo*. B6D2F1 mice (H-2^{bxd}) were reconstituted with B6-derived TCD-BM alone (H-2^b) or together with B6-derived spleen cells (H-2^b) and were co-injected with the P815 mastocytoma tumor cell line (H-2^d). RAPA or PBS was administered as described

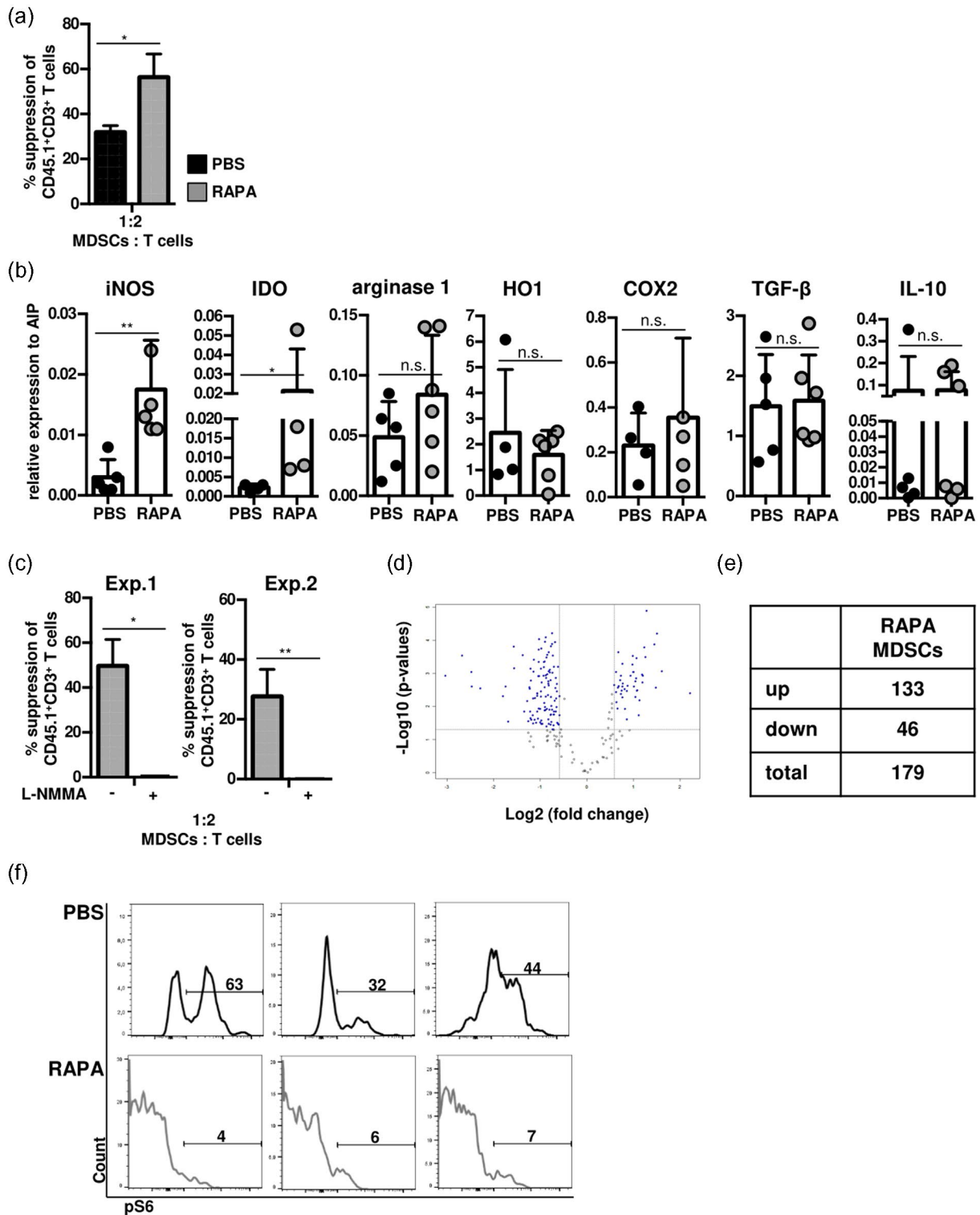


Fig. 5. Myeloid-derived suppressor cells (MDSCs) exhibit increased immunosuppressive potential and changes in gene expression after rapamycin (RAPA) treatment. (a–f) Lethally irradiated B6D2F1-recipient mice (H-2^{bxd}) were reconstituted with T cell depletion bone marrow (TCD-BM) from B6 mice (H-2^b) together with B6-derived spleen cells (SCs). RAPA or phosphate-buffered saline (PBS) intraperitoneal (i.p.) injections were administered every second day until day 10 post-transplantation. (a) Splenic MDSCs isolated from PBS and RAPA-treated mice were co-cultured with carboxyfluorescein diacetate succinimidyl ester (CFSE)-labeled B6.SJL-derived spleen cells (CD45.1, H-2^b) stimulated with irradiated allogeneic B6D2F1 (CD45.2, H-2^{bxd}) spleen cells. After 4 days, cells were stained for CD45.1 and CD3 and suppression of CD45.1⁺CD3⁺ T cell proliferation was determined. (b) MDSCs were analyzed for the expression of immunosuppressive factors by quantitative reverse transcription–polymerase chain reactions (qRT–PCRs) and relative expression to aryl hydrocarbon receptor-interacting protein (AIP) was calculated. (c) MDSCs isolated from RAPA-treated mice were co-cultured with CFSE-labeled B6.SJL-derived spleen cells (CD45.1, H-2^b) stimulated with irradiated allogeneic B6D2F1 (CD45.2, H-2^{bxd}) spleen cells in the presence or absence of the inducible nitric oxide synthase (iNOS) inhibitor L-NMMA. After 4 days, suppression of CD45.1⁺CD3⁺ T cell proliferation was determined. (d) Volcano plot comparing gene expression of *ex-vivo*-isolated MDSCs from RAPA or PBS-treated mice. Blue dots represent genes scored as differentially expressed between both groups. They display large magnitude fold changes (*x*-axis) and high statistical significance [$-\log_{10}$ of *P*-value (*y*-axis)]. Unfilled black dots show genes having a *P*-value > 0.05 and fold change less than 2 ($\log_2 = 1$). (e) Numbers of genes that were up- or down-regulated in MDSCs from RAPA-treated mice. (f) Five days after transplantation, MDSCs were isolated from BM transplanted mice and were stained for pS6 1 h after the last RAPA or PBS application. (a) Data represent the mean value \pm standard deviation (s.d.) of five performed experiments. Student's *t*-test. (b) Data represent the mean value \pm s.d. of *n* = 4–6 mice. Mann–Whitney test. (c) Data represent the mean value \pm s.d. of triplicates of two independent performed experiments. Student's *t*-test. (d,e) Data are the mean of three analyzed mice/group. (f) Fluorescence activated cell sorting (FACS) diagrams of *n* = 3 mice/group are shown. **P* \leq 0.05; ***P* \leq 0.01; n.s. = not significant.

Table 1. Top 10 of enriched GO terms in RAPA-activated MDSCs

	GO ID	GO term	% changed	<i>P</i> -value changed	Target genes
1.	71221	Cellular response to bacterial lipopeptide	40.0	2.0E-03	TLR1, CD36
2.	71220	Cellular response to bacterial lipoprotein		2.0E-04	
3.	70339	Response to bacterial lipopeptide		2.0E-04	
4.	32493	Response to bacterial lipoprotein		2.0E-04	
5.	77039	Cellular response to lipoteichoic acid	28.6	5.0E-04	CD36, CD14
6.	71223	Response to lipoteichoic acid		5.0E-04	
7.	43619	Regulation of transcription from RNA polymerase II promoter in response to oxidative stress	28.6	5.0E-04	HMOX1, CD36
8.	60670	Branching involved in labyrinthine layer morphogenesis	25.0	7.0E-04	SOCS3
9.	42613	MHC class II protein complex	25.0	7.0E-04	SPINT1
10.	19934	cGMP-mediated signaling	25.0	7.0E-04	H2-DMA, H2-OA CD36, EDNRB

Target genes up-regulated in rapamycin (RAPA)-activated myeloid-derived suppressor cells (MDSCs) compared to phosphate-buffered saline (PBS)-MDSCs are displayed in red, while down-regulated target genes are displayed in green.

MHC = major histocompatibility complex.

previously. PBS-treated recipient mice reconstituted with TCD-BM alone died from tumor development within 3 weeks after transplantation (Fig. 6c) due to massive tumor formation in spleen and liver reflected by elevated organ weights (Fig. 6d) and enrichment of H-2^d single-positive tumor cells (Fig. 6e). RAPA treatment alone could not abrogate tumor growth, as 90% of the RAPA-receiving mice reconstituted with TCD-BM in the absence of allogeneic spleen cells died from tumor development. Most importantly, RAPA treatment maintained the GVT effect in mice reconstituted with TCD-BM and allogeneic spleen cells. All surviving mice were tumor-free (Fig. 6c–e). Some mice reconstituted with TCD-BM and allogeneic spleen cells died despite RAPA treatment due to GVHD development reflected by increased GVHD scores (data not shown) and the absence of tumor cells in spleen and liver. Although PBS-treated mice

receiving TCD-BM and SC were tumor-free, approximately 90% of these mice developed lethal GVHD (Fig. 6c–e). In summary, these data clearly show that RAPA treatment strongly attenuates GVHD development after allogeneic BMT, which is associated with enhanced MDSC functions while simultaneously preserving T cell functions.

Discussion

Rapamycin and MDSCs both exhibit immunosuppressive functions and are applied in experimental BMT models or the clinics to prevent GVHD; however, their mutual influence is currently not well defined. In the current study, we confirmed that RAPA successfully alleviates GVHD development in a parent into F1 BMT mouse model with MHC classes I and II disparities of 50%. To

our knowledge, we show here for the first time that RAPA treatment in the context of BMT enhanced the immunosuppressive function of MDSCs and significantly changed their genomic landscape. Most importantly, RAPA treatment does not significantly affect the T cell compartment

on genomic and functional levels, whereby T cell immunity and anti-tumor cytotoxicity were maintained.

Pilot studies of Blazer *et al.* [38,39] demonstrated that RAPA inhibits GVHD development in experimental BMT models; however, the underlying mechanism is still not

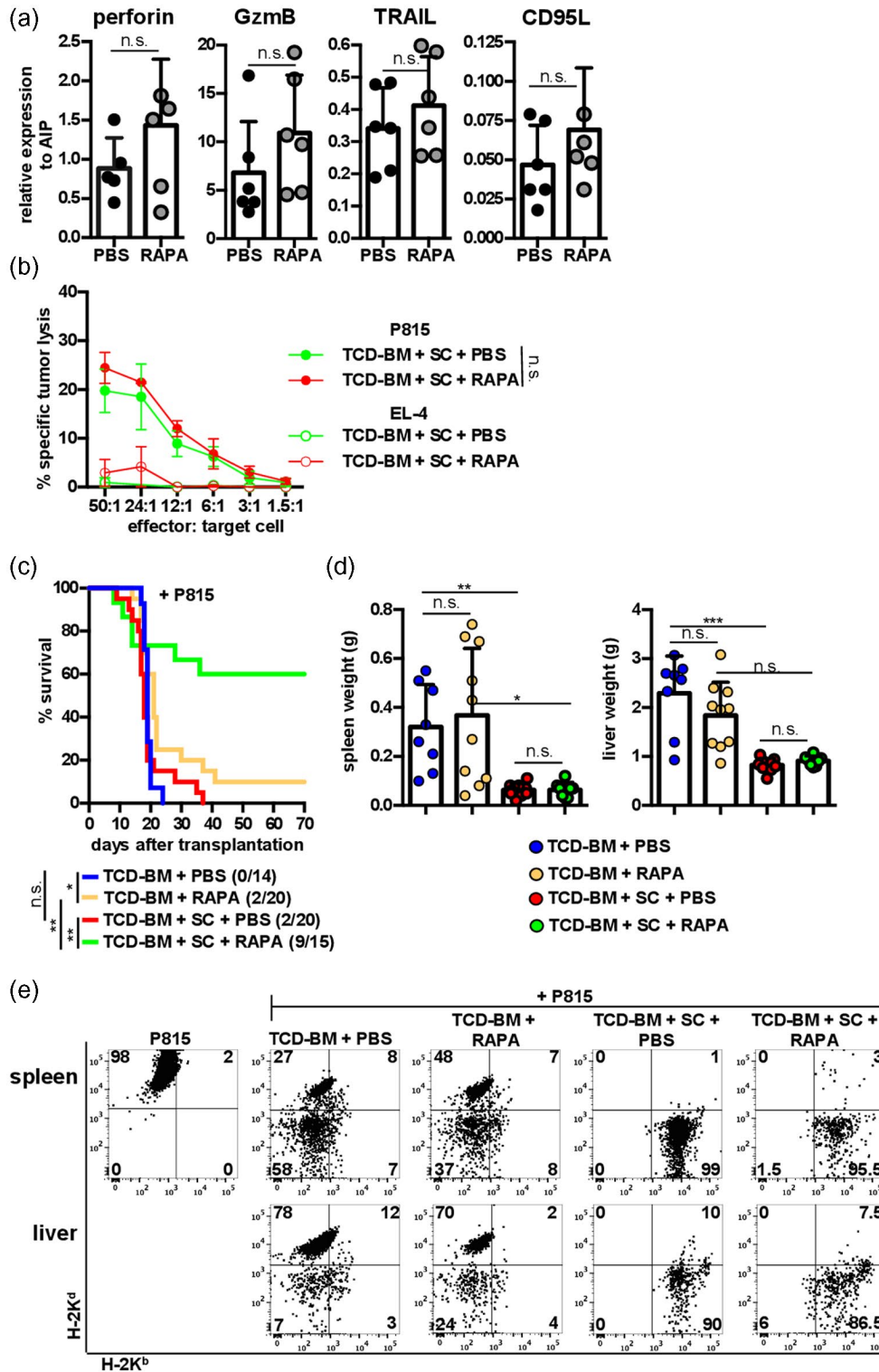


Fig. 6. T cell cytotoxicity and the graft-versus-tumor (GVT) effect are maintained under rapamycin (RAPA) treatment. (a–e) Lethally irradiated B6D2F1 recipient mice (H-2^{bxd}) were reconstituted with T cell depletion bone marrow (TCD-BM) from B6 mice (H-2^b) and B6-derived spleen cells (SCs). RAPA or phosphate-buffered saline (PBS) intraperitoneal (i.p.) injections were administered every second day during the first 10 days, followed by a treatment twice weekly until the end of the experiment. (a) Splenic CD3⁺ T cells were isolated 10 days after bone marrow transplant (BMT). Quantitative reverse transcription–polymerase chain reaction (qRT–PCR) analyses of cytotoxic molecules were performed and relative expression to aryl hydrocarbon receptor-interacting protein (AIP) was calculated. (b) Spleen cells (H-2^b) of RAPA or PBS-treated mice were co-cultured with ⁵¹Cr-labeled P815 (H-2^d) or EL-4 (H-2^b) tumor cells and specific tumor lysis was determined. (c–e) Additionally, P815 tumor cells (H-2^d) were co-injected at day of BMT. (c) Survival was determined. Surviving animals/total animals treated are indicated in brackets. (d) Spleen and liver weights were determined the day mice were euthanized due to their moribund state or at the end of the experiment. (e) Presence of tumor cells was determined in spleens and livers by staining for H-2K^b and H-2K^d the day mice were euthanized due to their moribund state or at the end of the experiment. Fluorescence activated cell sorting (FACS) analyses are shown for one representative mouse/group. Data represent the mean value ± standard deviation (s.d.) of five to six mice/group (a) and seven to nine mice/group (d). (b) Data represent the mean value ± standard error of the mean (s.e.m.) of three mice/group. (a,b) Mann–Whitney test. (c) Kaplan–Meier method and log-rank test. (d) Kruskal–Wallis test. **P* ≤ 0.05; ***P* ≤ 0.01; ****P* ≤ 0.001; n.s. = not significant.

well defined. In a parent into F1 model (B6→B6D2F1), we could confirm that GVHD-induced mortality was reduced from 90 to 25–40% and histological GVHD was strongly attenuated under RAPA treatment. Lethal GVHD in this model depends upon the presence of mature CD4⁺ T cells in the transplant. Initially the effect of RAPA was referred to preferential inhibition of CD8⁺ T cells [39], but the effectiveness of RAPA in CD4-dependent GVHD models was also confirmed by using various donor/recipient combinations [11,40,41].

RAPA effects are largely attributed to its ability to block T cell activation and proliferation. However, even in the early phase of GVHD, where massive expansion of allogeneic T cells occurs, we observed an increase in splenocyte numbers including CD4⁺ and CD8⁺ T cells. Accordingly, activated CD44⁺ or memory CD44⁺CD122⁺ T cells from which most of them represent effector memory T cells were equally present in RAPA and PBS-treated animals. Differences in the expression of adhesion and homing molecules, exhaustion markers and cytokine profiles were not found in T cells isolated from RAPA- or PBS-treated mice. Most importantly, gene array analysis revealed no significant differences in T cell gene expression profiles between RAPA and PBS-treated mice.

In a fully MHC mismatched BMT model, RAPA was reported to diminish allogeneic T cell expansion early after transplantation *in vivo*. However, these cells preserved their proliferative capacity towards allogeneic stimulation *in vitro*, although reduction in IFN- γ and GzmB and GzmA levels indicate a skewing of T cells towards Th2/Tc2 cells [39]. Applying RAPA together with Th2 polarizing cytokines also induces Th2 cells *in vitro* which, after adoptive transfer, prevented GVHD [42]. However, this approach is flexible and depends upon the cytokines used, as RAPA in the presence of IL-2, -7 and -12 supports Th1 polarization [43]. Most interestingly, T cells that are polarized in the presence of RAPA exhibit increased effector functions with improved

CD8⁺ T cell immunity leading to enhanced tumor reactivity [44]. In our studies, cytolytic functions of *ex-vivo*-isolated allogeneic T cells from BM-transplanted mice under RAPA treatment were comparable to T cells from PBS-treated animals. Consistently, the GVT effect was maintained and mice receiving allogeneic splenocytes and RAPA treatment were all tumor-free. Although direct anti-leukemic effects of RAPA are reported *in vitro* [45], RAPA treatment in the absence of allogeneic T cells could not prevent the development of tumors, but slightly prolonged the time until tumor developed. A previously published study using a combination of RAPA and bortezomib for GVHD prophylaxis also showed efficient anti-leukemic cytotoxicity, although the effect of the single drugs was not investigated [46]. In contrast, when donor lymphocytes were infused 2 weeks after BMT followed directly by leukemia challenge, RAPA treatment starting on the day of donor lymphocyte infusion (DLI) abrogated the protective effect of DLI and mice succumbed to cancer [39].

As the major therapeutic effect of RAPA was not attributed to T cells, alterations in the induction and function of immunoregulatory cells were investigated. As shown previously and confirmed by our data, induction of T_{regs} is not impaired under RAPA treatment due to their relative independence on mTOR activation [47–49]. Accumulation of T_{regs} in the skin of RAPA-treated BMT mice was observed when high doses of 3–5 mg/kg were administered [40], but not at doses of 1.5 mg/kg, which are applied in our studies. Splenic MDSCs increased under RAPA therapy, but the ratio of T cells to MDSCs remained constant. However, *ex-vivo*-isolated MDSCs exhibited an increased immunosuppressive potential in MLRs. This was accompanied by a significant increase in iNOS expression and up-regulation of arginase 1 and IDO. An activating effect of RAPA on MDSCs induction and function was noticed in different murine models of kidney and liver inflammation or solid organ transplantation. mTOR deficiency by RAPA treatment recruits MDSCs into inflamed

livers or kidneys or supports the migration of MDSCs into cardiac allografts, thereby ameliorating disease [9,10,12,13]. Depending on the model used, immunosuppressive capacity of MDSCs was continuously dependent upon iNOS expression, while arginase-1 expression strengthens the effect in some models. Most importantly, in contrast to allogeneic T cells the genomic landscape of MDSCs was significantly changed by RAPA treatment. GO term analysis revealed enrichment in target genes associated with uptake or cellular responses to lipopeptides, lipoproteins and lipoteichoic acids in RAPA-activated MDSCs. These data support recently published studies showing that elevated lipid contents augment the immunosuppressive function of MDSCs [50–52].

Few studies also report the requirement of mTOR activation for MDSC functionality. The activation of the AKT/mTOR pathway by granulocyte antigen-colony-stimulating factor (GM-CSF) is a prerequisite to convert murine and human monocytes from inflammatory cells into suppressor cells [16]. Similarly, glycolysis-mediated immunosuppression of tumor-associated monocytic MDSCs can be abrogated by mTOR inhibition [15,17]. It is noteworthy that impaired MDSC function due to mTOR inhibition is attributed only to immunosuppressive cells of the monocytic lineage, while activating effects after mTOR impairment is observed in unseparated or granulocytic MDSCs. Thus, the adoptive transfer of granulocytic MDSCs isolated from *in-vitro* cultures of RAPA-treated BM cells prevents GVHD [11].

To our knowledge, there are currently no clinical data available for the mutual interference of RAPA (sirolimus) and MDSCs. This might be due to the fact that human MDSCs still cannot be defined solely by surface markers and that sirolimus is not generally applied as first-line monotherapy, but mainly in combination with calcineurin inhibitors or together with mycophenolate mofetil and cyclophosphamide [24].

With our study we provide the first indications that RAPA might be applicable in clinical situations where the immunosuppressive capacity of MDSCs needs to be strengthened without impairing T cell-mediated immunity.

Acknowledgements

The authors thank Linda Wolf and Ingrid Knape (Department of Pediatrics and Adolescent Medicine) for excellent technical assistance. This study was supported by the Deutsche José Carreras Leukämie-Stiftung e.V. (DJCLS F13/04), Boehringer Ingelheim Ulm University BioCenter (TPI2) and the International Graduate School in Molecular Medicine, Ulm, Germany. Open access funding enabled and organized by Projekt DEAL.

Disclosures

All authors declare no competing financial and commercial interests.

Author contributions

J. S., T. R., F. L., J. J. M. and K. H. performed experiments and analysed data. J. S. generated the figures. K.-M. D. contributed to the study design and interpreted data. G. S. created the study design, performed data interpretation and wrote the manuscript together with J. S. All authors approved the final version of the manuscript, revised the manuscript and are accountable for all respects of the work.

Data availability statement

The data that support the findings of this study are available from the corresponding author (Gudrun.strauss@uniklinik-ulm.de) upon reasonable request.

References

- 1 Markey KA, MacDonald KP, Hill GR. The biology of graft-versus-host disease: experimental systems instructing clinical practice. *Blood* 2014; **124**:354–62.
- 2 Saxton RA, Sabatini DM. mTOR signaling in growth, metabolism, and disease. *Cell* 2017; **168**:960–76.
- 3 Sarbassov DD, Ali SM, Sengupta S *et al.* Prolonged rapamycin treatment inhibits mTORC2 assembly and Akt/PKB. *Mol Cell* 2006; **22**:159–68.
- 4 Delgoffe GM, Kole TP, Zheng Y *et al.* The mTOR kinase differentially regulates effector and regulatory T cell lineage commitment. *Immunity* 2009; **30**:832–44.
- 5 Rao RR, Li Q, Odunsi K, Shrikant PA. The mTOR kinase determines effector versus memory CD8+ T cell fate by regulating the expression of transcription factors T-bet and Eomesodermin. *Immunity* 2010; **32**:67–78.
- 6 Thomson AW, Turnquist HR, Raimondi G. Immunoregulatory functions of mTOR inhibition. *Nat Rev Immunol* 2009; **9**:324–37.
- 7 Battaglia M, Stabilini A, Roncarolo MG. Rapamycin selectively expands CD4+CD25+FoxP3+ regulatory T cells. *Blood* 2005; **105**:4743–8.
- 8 Haxhinasto S, Mathis D, Benoist C. The AKT-mTOR axis regulates de novo differentiation of CD4+Foxp3+ cells. *J Exp Med* 2008; **205**:565–74.
- 9 Zhang Y, Bi Y, Yang H *et al.* mTOR limits the recruitment of CD11b+Gr1+Ly6Chigh myeloid-derived suppressor cells in protecting against murine immunological hepatic injury. *J Leukoc Biol* 2014; **95**:961–70.
- 10 Nakamura T, Nakao T, Yoshimura N, Ashihara E. Rapamycin prolongs cardiac allograft survival in a mouse model by inducing

- myeloid-derived suppressor cells. *Am J Transplant* 2015; **15**:2364–77.
- 11 Lin Y, Wang B, Shan W *et al.* mTOR inhibitor rapamycin induce polymorphonuclear myeloid-derived suppressor cells mobilization and function in protecting against acute graft-versus-host disease after bone marrow transplantation. *Clin Immunol* 2018; **187**:122–31.
 - 12 Zhang C, Wang S, Li J *et al.* The mTOR signal regulates myeloid-derived suppressor cells differentiation and immunosuppressive function in acute kidney injury. *Cell Death Dis* 2017; **8**:e2695.
 - 13 Wei C, Wang Y, Ma L *et al.* Rapamycin nano-micelle ophthalmic solution reduces corneal allograft rejection by potentiating myeloid-derived suppressor cells' function. *Front Immunol* 2018; **9**:2283.
 - 14 Ding X, Du H, Yoder MC, Yan C. Critical role of the mTOR pathway in development and function of myeloid-derived suppressor cells in *lal^{-/-}* mice. *Am J Pathol* 2014; **184**:397–408.
 - 15 Wu T, Zhao Y, Wang H *et al.* mTOR masters monocytic myeloid-derived suppressor cells in mice with allografts or tumors. *Sci Rep* 2016; **6**:20250.
 - 16 Ribechini E, Hutchinson JA, Hergovits S *et al.* Novel GM-CSF signals via IFN- γ /IRF-1 and AKT/mTOR license monocytes for suppressor function. *Blood Adv* 2017; **1**:947–60.
 - 17 Deng Y, Yang J, Luo F *et al.* mTOR-mediated glycolysis contributes to the enhanced suppressive function of murine tumor-infiltrating monocytic myeloid-derived suppressor cells. *Cancer Immunol Immunother* 2018; **67**:1355–64.
 - 18 Gabrilovich DI, Nagaraj S. Myeloid-derived suppressor cells as regulators of the immune system. *Nat Rev Immunol* 2009; **9**:162–74.
 - 19 Veglia F, Perego M, Gabrilovich D. Myeloid-derived suppressor cells coming of age. *Nat Immunol* 2018; **19**:108–19.
 - 20 Groth C, Hu X, Weber R *et al.* Immunosuppression mediated by myeloid-derived suppressor cells (MDSCs) during tumour progression. *Br J Cancer* 2019; **120**:16–25.
 - 21 Klintmalm GB, Nashan B. The Role of mTOR Inhibitors in Liver Transplantation: Reviewing the Evidence. *J Transplant* 2014; **2014**:845438.
 - 22 Johnson RW. Sirolimus (Rapamune) in renal transplantation. *Curr Opin Nephrol Hypertens* 2002; **11**:603–7.
 - 23 Moes DJ, Guchelaar HJ, de Fijter JW. Sirolimus and everolimus in kidney transplantation. *Drug Discov Today* 2015; **20**:1243–9.
 - 24 Lutz M, Mielke S. New perspectives on the use of mTOR inhibitors in allogeneic haematopoietic stem cell transplantation and graft-versus-host disease. *Br J Clin Pharmacol* 2016; **82**:1171–9.
 - 25 Messmann JJ, Reisser T, Leithauser F, Lutz MB, Debatin K-M, Strauss G. *In vitro*-generated MDSCs prevent murine GVHD by inducing type 2 T cells without disabling antitumor cytotoxicity. *Blood* 2015; **126**:1138–48.
 - 26 Park MY, Lim BG, Kim S-Y, Sohn H-J, Kim S, Kim T-G. GM-CSF promotes the expansion and differentiation of cord blood myeloid-derived suppressor cells, which attenuate xenogeneic graft-vs.-host disease. *Front Immunol* 2019; **10**:183.
 - 27 Wang K, Lv M, Chang YJ *et al.* Early myeloid-derived suppressor cells (HLA-DR(-)/(low)CD33(+)/CD16(-)) expanded by granulocyte colony-stimulating factor prevent acute graft-versus-host disease (GVHD) in humanized mouse and might contribute to lower GVHD in patients post allo-HSCT. *J Hematol Oncol* 2019; **12**:31.
 - 28 Rieber N, Wecker I, Neri D *et al.* Extracorporeal photopheresis increases neutrophilic myeloid-derived suppressor cells in patients with GvHD. *Bone Marrow Transplant* 2014; **49**:545–52.
 - 29 Fan Q, Liu H, Liang X *et al.* Superior GVHD-free, relapse-free survival for G-BM to G-PBSC grafts is associated with higher MDSCs content in allografting for patients with acute leukemia. *J Hematol Oncol* 2017; **10**:135.
 - 30 Luyckx A, Schoupe E, Rutgeerts O *et al.* Subset characterization of myeloid-derived suppressor cells arising during induction of BM chimerism in mice. *Bone Marrow Transplant* 2012; **47**:985–92.
 - 31 Wang D, Yu Y, Haarberg K *et al.* Dynamic change and impact of myeloid-derived suppressor cells in allogeneic bone marrow transplantation in mice. *Biol Blood Marrow Transplant* 2013; **19**:692–702.
 - 32 Cooke KR, Kobzik L, Martin TR *et al.* An experimental model of idiopathic pneumonia syndrome after bone marrow transplantation: I. The roles of minor H antigens and endotoxin. *Blood* 1996; **88**:3230–9.
 - 33 Kaplan DH, Anderson BE, McNiff JM, Jain D, Shlomchik MJ, Shlomchik WD. Target antigens determine graft-versus-host disease phenotype. *J Immunol* 2004; **173**:5467–75.
 - 34 Strauss G, Knape I, Melzner I, Debatin K-M. Constitutive caspase activation and impaired death-inducing signaling complex formation in CD95-resistant, long-term activated, antigen-specific T cells. *J Immunol* 2003; **171**:1172–82.
 - 35 Irizarry RA, Hobbs B, Collin F *et al.* Exploration, normalization, and summaries of high density oligonucleotide array probe level data. *Biostatistics* 2003; **4**:249–64.
 - 36 Benjamini Y, Yosef H. Controlling the false discovery rate: a practical and powerful approach to multiple testing. *J R Stat Soc B* 1995; **57**:249–64.
 - 37 Szklarczyk D, Franceschini A, Wyder S *et al.* STRING v10: protein–protein interaction networks, integrated over the tree of life. *Nucleic Acids Res* 2015; **43**:D447–452.
 - 38 Blazar BR, Taylor PA, Snover DC, Sehgal SN, Vallera DA. Murine recipients of fully mismatched donor marrow are protected from lethal graft-versus-host disease by the *in vivo* administration of rapamycin but develop an autoimmune-like syndrome. *J Immunol* 1993; **151**:5726–41.
 - 39 Blazar BR, Taylor PA, Panoskaltis-Mortari A, Vallera DA. Rapamycin inhibits the generation of graft-versus-host disease- and graft-versus-leukemia-causing T cells by interfering with the production of Th1 or Th1 cytotoxic cytokines. *J Immunol* 1998; **160**:5355–65.

- 40 Palmer JM, Chen BJ, DeOliveira D, Le ND, Chao NJ. Novel mechanism of rapamycin in GVHD: increase in interstitial regulatory T cells. *Bone Marrow Transplant* 2010; **45**: 379–84.
- 41 Satake A, Schmidt AM, Nomura S, Kambayashi T. Inhibition of calcineurin abrogates while inhibition of mTOR promotes regulatory T cell expansion and graft-versus-host disease protection by IL-2 in allogeneic bone marrow transplantation. *PLOS ONE* 2014; **9**:e92888.
- 42 Foley JE, Jung U, Miera A *et al.* *Ex vivo* rapamycin generates donor Th2 cells that potently inhibit graft-versus-host disease and graft-versus-tumor effects via an IL-4-dependent mechanism. *J Immunol* 2005; **175**:5732–43.
- 43 Jung U, Foley JE, Erdmann AA *et al.* *Ex vivo* rapamycin generates Th1/Tc1 or Th2/Tc2 Effector T cells with enhanced *in vivo* function and differential sensitivity to post-transplant rapamycin therapy. *Biol Blood Marrow Transplant* 2006; **12**: 905–18.
- 44 Li Q, Rao RR, Araki K *et al.* A central role for mTOR kinase in homeostatic proliferation induced CD8+ T cell memory and tumor immunity. *Immunity* 2011; **34**:541–53.
- 45 Recher C, Beyne-Rauzy O, Demur C *et al.* Antileukemic activity of rapamycin in acute myeloid leukemia. *Blood* 2005; **105**:2527–34.
- 46 Caballero-Velazquez T, Sanchez-Abarca LI, Gutierrez-Cosio S *et al.* The novel combination of sirolimus and bortezomib prevents graft-versus-host disease but maintains the graft-versus-leukemia effect after allogeneic transplantation. *Haematologica* 2012; **97**:1329–37.
- 47 Zeiser R, Leveson-Gower DB, Zambricki EA *et al.* Differential impact of mammalian target of rapamycin inhibition on CD4+CD25+Foxp3+ regulatory T cells compared with conventional CD4+ T cells. *Blood* 2008; **111**:453–62.
- 48 Sugiyama H, Maeda Y, Nishimori H *et al.* Mammalian target of rapamycin inhibitors permit regulatory T cell reconstitution and inhibit experimental chronic graft-versus-host disease. *Biol Blood Marrow Transplant* 2014; **20**:183–91.
- 49 Coenen JJ, Koenen HJ, van Rijssen E *et al.* Rapamycin, not cyclosporine, permits thymic generation and peripheral preservation of CD4+ CD25+ FoxP3+ T cells. *Bone Marrow Transplant* 2007; **39**:537–45.
- 50 Veglia F, Tyurin VA, Blasi M *et al.* Fatty acid transport protein 2 reprograms neutrophils in cancer. *Nature* 2019; **569**:73–8.
- 51 Al-Khami AA, Zheng L, Del Valle L *et al.* Exogenous lipid uptake induces metabolic and functional reprogramming of tumor-associated myeloid-derived suppressor cells. *Oncoimmunology* 2017; **6**:e1344804.
- 52 Hossain F, Al-Khami AA, Wyczzechowska D *et al.* Inhibition of fatty acid oxidation modulates immunosuppressive functions of myeloid-derived suppressor cells and enhances cancer therapies. *Cancer Immunol Res* 2015; **3**:1236–47.

Supporting Information

Additional Supporting Information may be found in the online version of this article at the publisher's web site:

Fig. S1. Lethally irradiated B6D2F1 recipient mice (H-2bxd) were reconstituted with T cell depleted bone marrow from B6 mice (H-2b) together with B6-derived spleen cells. Rapamycin (RAPA) or PBS i.p. injections were administered every second day until day 10 post-transplantation. (a) Total MDSCs in spleen and liver were defined by CD11b and Gr-1 expression. (b) Spleen and livers were analyzed for Tregs by analysing CD4+ CD25+ cells for FoxP3 expression. (c) Granulocytic (CD11b+Ly-GhighLy-6Clow) and monocytic MDSC subsets (CD11b+Ly-6GnegLy-6Chigh) were defined in spleen and liver by analyzing CD11b+ cells for their expression of Ly-6C and Ly-6G. (a) FACS diagrams show one representative mouse out of 12 mice analyzed/group. (b) FACS diagrams show one representative mouse out of 5–6 mice analyzed/group. (c) FACS diagrams show one representative mouse out of 6 mice analyzed/group.

Fig. S2. Lethally irradiated B6D2F1 recipient mice (H-2bxd) were reconstituted with T cell depleted bone marrow from B6 mice (H-2b) together with B6-derived spleen cells. Rapamycin (RAPA) or PBS i.p. injections were administered every second day. 10 days after transplantation, splenic CD4+ and CD8+ T cells were stained for different activation, homing and adhesion markers. MFI of each marker was defined. Data represent the mean value \pm SD of 3 mice/group. Mann-Whitney test. n.s. = not significant.

Fig. S3. Lethally irradiated B6D2F1 recipient mice (H-2bxd) were reconstituted with T cell depleted bone marrow from B6 mice (H-2b) together with B6-derived spleen cells. Rapamycin (RAPA) or PBS i.p. injections were administered until day 5 post-transplantation. One h after the last application, splenic T cells were stained for CD3 and phospho-S6 ribosomal protein expression was determined on CD3+ T cells. (a) FACS diagrams of one representative mouse/group out of 3 analyzed mice/group are shown. (b) Data represent the mean value \pm SD of 3 mice/group. Mann-Whitney test. n.s. = not significant.

Table S1. Antibodies for flow cytometry.

Table S2. Primer for qRT-PCR.

Table S3. Differentially expressed genes in T cells upon rapamycin treatment compared to PBS treatment.